Zahra Mardani*, Samira Akbari, Keyvan Moeini, Majid Darroudi, Cameron Carpenter-Warren, Alexandra M. Z. Slawin and J. Derek Woollins

2D-Coordination polymer containing lead(II) in a hemidirected PbO_4S_3 environment formed by molecular breaking of the 1,3-oxathiolane ligand

https://doi.org/10.1515/znb-2019-0043
Received February 4, 2019; accepted June 23, 2019

Abstract: A new 1,3-oxathiolane-based ligand, 2-(1,3-oxathiolan-2-yl)pyridine, was prepared and its coordination to lead(II) was investigated. Experiments revealed a ligand-breaking reaction during the complexation process, which leads to the formation of a 2D-coordination polymer of lead(II), $[Pb(\mu^3\text{-HME})(\mu\text{-OAc})]_n$; H_2ME: 2-mercaptoethanol. The compounds have been characterized by elemental analysis, FT-IR, ^1H NMR spectroscopy and single-crystal X-ray diffraction. X-ray analysis revealed a 2D-coordination polymer extending via acetato bridges. The lead(II) center adopts a rare PbO_4S_3-distorted pentagonal bipyramidal geometry with a hemidirected arrangement. Upon coordination, the thiol group of the H_2ME ligand is deprotonated to coordinate as an anionic ligand. The network extends in sheets in the crystallographic *ab* plane via Pb–S–Pb and Pb–O–Pb bridges, aided by O–H···O hydrogen bonds.

Keywords: 2-mercaptoethanol; coordination polymer; hemidirected coordination sphere; lead(II); molecular breaking.

1 Introduction

Coordination polymers have interesting molecular architectures, and potential applications in the fields of functional materials [1], electrical conductivity [2], ion exchange [3], nonlinear optics [4], selective catalysis [5], gas storage/separation and ion exchange [6–11], biological and material science [12, 13], precursors for the preparation of nano-materials [14] and magnetism [15–19] have been proposed.

Lead(II) is particularly attractive in coordination chemistry, since the different geometries adopted by its complexes allow a degree of tolerance for ligand configuration that is not exhibited, for example, by *d*-block elements [20, 21]. These features permit lead to bind both hard and soft donor atoms forming compounds of different structural types and with unusual architectures which, sometimes, might not be expected. Lead(II)-based inorganic–organic hybrid materials have captured the interests of chemists due to their diverse structural motifs [22] and fascinating optical/electronic properties such as photoluminescence [23], nonlinear optics [24], semiconductivity [25] and dielectric behaviors [26]. Specially, their applications in light emitting diodes [27] and solar cells [28] have become a hot field recently.

In order to extend the chemistry of the coordination polymers of lead, this work describes the coordination of a new 1,3-oxathiolane derivative, 2-(1,3-oxathiolan-2-yl) pyridine (OTP, Scheme 1), to lead(II) acetate. Based on the X-ray analysis, the OTP ligand is broken during the complexation process to form 2-mercaptoethanol (H_2ME), ultimately resulting in a 2D coordination polymer of $[Pb(\mu^3\text{-HME})(\mu\text{-OAc})]_n$ (**1**). The OTP ligand and its lead(II) complex have been characterized by elemental analysis, FT-IR and ^1H NMR spectroscopy, and single-crystal X-ray diffraction (only **1**).

2 Results and discussions

2-Mercaptoethanol was reacted with picolinaldehyde under solvent-free conditions using ultrasonic irradiation to give the OTP ligand via an oxathiolanation reaction (Scheme 1). This OTP was then reacted with $Pb(OAc)_2 \cdot 3H_2O$

***Corresponding author: Zahra Mardani,** Inorganic Chemistry Department, Faculty of Chemistry, Urmia University, 57561-51818 Urmia, I.R. Iran, e-mail: z.mardani@urmia.ac.ir
Samira Akbari: Inorganic Chemistry Department, Faculty of Chemistry, Urmia University, 57561-51818 Urmia, I.R. Iran
Keyvan Moeini: Chemistry Department, Payame Noor University, 19395-4697 Tehran, I.R. Iran
Majid Darroudi: Nuclear Medicine Research Center, Mashhad University of Medical Sciences, 99191-91778 Mashhad, I.R. Iran
Cameron Carpenter-Warren, Alexandra M. Z. Slawin and J. Derek Woollins: EaStCHEM School of Chemistry, University of St Andrews, St Andrews, Fife KY16 9ST, UK

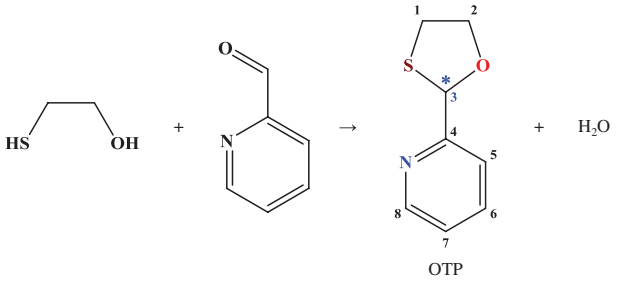

Scheme 1: The synthetic route to the 2-(1,3-oxathiolan-2-yl)pyridine ligand with atom numbering.

in branched tubes to give the 2D coordination polymer of **1** in which the OTP ligand is converted to the HME^- anion. Similar structural conversion of the ligand during the complexation process was observed for an oxazolidine ligand [29, 30].

2.1 Spectroscopic studies

In the FT-IR spectrum of OTP, the presence of the aromatic and aliphatic C–H stretching vibrations confirms the successful condensation of 2-mercaptoethanol with picolinaldehyde. In the FT-IR spectrum of **1**, a ν (O–H) band is observed, which can be attributed to the degradation of the OTP ligand to its precursors. The pyridine ring in the structure of OTP leads to bands at 1589 cm^{-1} for the ν (C=N) and at 750 and 700 cm^{-1} for the ring wagging vibrations [31, 32].

In the FT-IR spectrum of **1**, three bands at 1543, 1410 and 660 cm^{-1} can be assigned to ν_{as} (COO), ν_s (COO) and δ (OCO), respectively [33], confirming the presence of the acetate unit in this complex. The differences between the asymmetric (ν_{as}) and the symmetric (ν_s) stretching of the acetate group (Δ) can reveal its coordination type. Compared to the value for the acetate salt, monodentate complexes exhibit much larger Δ values (164 cm^{-1}), whilst in bidentate complexes these values are significantly lower than this [34, 35]. The Δ value for **1** is 133 cm^{-1}, which corresponds to bidentate acetate coordination.

In the ^1H NMR spectrum of the OTP ligand (see Scheme 1 for numbering), there are three sets of signals: a series of multiplets in the aromatic region at 7–9 ppm, a singlet at 5.92 ppm corresponding to the H atom at the chiral carbon atom and two triplets in the downfield region related to the CH_2–CH_2 group of the 2-mercaptoethanol unit.

2.2 Crystal and molecular structure of [Pb(μ3-HME)(μ-OAc)]n

X-ray structure analysis of **1** (Fig. 1) reveals a 2D coordination polymer extending in the crystallographic *ab* plane. Each lead(II) center has a PbO_4S_3 hemidirected environment, with the 7-coordinate geometry best being described as distorted pentagonal bipyramidal. Each Pb center is chelated by an acetate group, both oxygen atoms (O2, O3) of which are also bridging to neighboring Pb atoms. The Pb atom is further O,S-chelated by an HME^- ligand (O1 and S1 in Fig. 1), the S atom of which is triply bridging three Pb atoms. Conversely, each Pb atom connects to three S atoms. These are known features in Pb(II) coordination chemistry [36, 37]. Among the four Pb–O bond lengths the $Pb–O^{bridging}$ (2.917(2) Å) is significantly longer than the others. Looking at a cross section of the sheets shows that the Pb and S atoms lie in the center of the layers, with the aliphatic units lining the outsides of each sheet, with no specific intra-sheet interactions present.

Searching the Cambridge Structural Database [38] has revealed that the PbO_4S_3 environment is rare and only one example has been reported [39].

The HME^- ligand acting as a bidentate O,S donor forms a five-membered nonplanar chelate ring, while the chelating acetate group forms a slightly folded

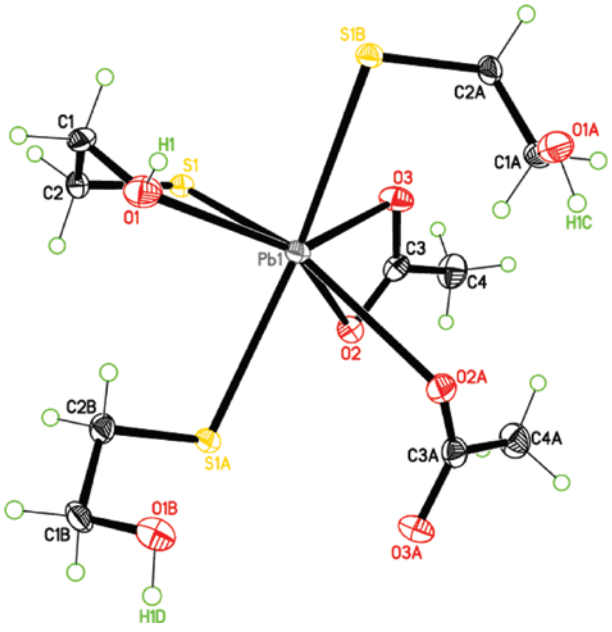

Fig. 1: A displacement ellipsoid plot of the coordination environment of the lead(II) center, showing displacement ellipsoids at the 50% probability level and hydrogen atoms drawn as spheres of arbitrary radius.

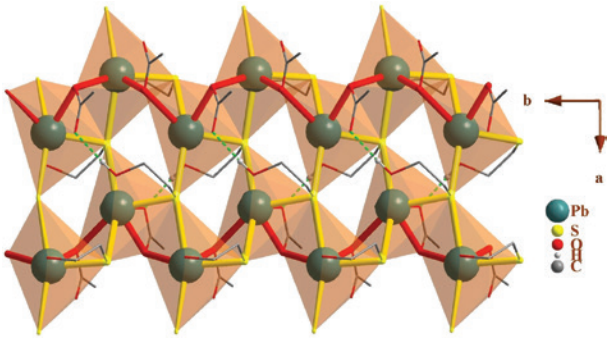

Fig. 2: Packing and crosslinking of molecules **1** in the crystal showing the hydrogen bonds. Each PbO_4S_3 unit is shown as a polyhedron. The connectivity of the polymeric chains is highlighted.

four-membered ring. The dihedral angle between mean planes through the four- and five-membered chelate rings is 87.32°, confirming that the acetate and HME^- ligands are perpendicular to each another. It is the thiol group of the H_2ME ligand which is deprotonated, rather than the alcohol group.

In complex **1**, the differences between the longest and the shortest four Pb–O (0.404 Å) and three Pb–S bond lengths (0.380 Å) are significant. This observation is typical for complexes with central atoms exhibiting lone pairs [40, 41]. Based on these observations, and the distorted geometry, we conclude that the coordination sphere around the lead atom can be described as hemidirected, but the effect is not really pronounced. In the structural network of **1** (Fig. 2), there are O–H···O hydrogen bonds originating from the dangling CH_2CH_2OH group, which strengthen in intra-sheet interactions.

3 Conclusion

In this work, a new 2D-coordination polymer of lead(II), $[Pb(\mu^3\text{-HME})(\mu\text{-OAc})]_n$; H_2ME: 2-mercaptoethanol, was synthesized in a reaction between lead acetate and an OTP ligand. The spectral (IR, ^1H NMR) and structural (X-ray) investigations revealed that upon coordination, the OTP ligand broke and produced the H_2ME ligand. The thiol group of this ligand became deprotonated and bound to the lead(II) ions. In **1**, the polymeric structure is extended by the bridging acetate ligands with a coordination mode of "(O,μ-O)" in one dimension, while the triply bridging thiolato groups generate sheets in the crystallographic *ab* plane. In this complex, the lead atom has a rare distorted pentagonal bipyramidal PbO_4S_3 environment with a hemidirected coordination sphere. Intra-sheet O–H···O hydrogen bonding is also present.

4 Experimental section

4.1 Materials and measurements

All starting chemicals and solvents were reagent or analytical grade and used as received. The infrared spectra of KBr pellets in the range 4000–400 cm^{-1} were recorded with an FT-IR TENSOR 27 spectrometer. ^1H NMR spectra were recorded on the Bruker Aspect 3000 instrument. The carbon, hydrogen and nitrogen contents were determined by a Thermo Finnigan Flash Elemental Analyzer 1112 EA. The melting points were determined with Barnsted Electrothermal 9200 electrically heated apparatus.

4.2 Preparation of 2-(1,3-oxathiolan-2-yl) pyridine (OTP)

2-Mercaptoethanol (1.55 g, 19.84 mmol) and picolinaldehyde (2.12 g, 19.79 mmol) were heated to 60°C in an ultrasonic bath for 2 h under solvent-free conditions, yielding dark brown oil. Precursors were removed by rotary evaporation. Yield: 3.09 g, 93%. – Analysis calcd. for C_8H_9NOS: C 57.46, H 5.42, N 8.38; found C 57.98, H 5.53, N 8.20%. –IR (KBr disk): $\nu = 3058$ m $(C–H)^{ar}$, $\nu_{as} = 2923$ m (CH_2), $\nu_s = 2876$ w (CH_2), $\nu = 1589$ s (C=N), 1468 m (C=C), $\delta_{as} = 1435$ s (CH_2), $\delta_s = 1358$ m (CH_2), $\nu = 1243$ s (C–O), $\gamma = 750$ s and 703 m (py), $\nu = 621$ m (C–S) cm^{-1}. –^1H NMR (300 MHz, [D_6] dimethyl sulfoxide (DMSO)): $\delta = 7.20–8.71$ (m, 4 H, $C^5H–C^8H$), 5.92 (s, 1 H, C^3H), 3.49 (t, 2 H, C^2H_2), 2.52 (t, 2 H, C^1H_2) ppm.

4.3 Preparation of [Pb(HME)(μ-OAc)]n

OTP (0.17 g, 1.02 mmol) and $Pb(OAc)_2 \cdot 3H_2O$ (0.20 g, 0.53 mmol) were placed in the large arms of a branched tube with a total capacity of 15 mL. Methanol was carefully added to fill both arms. The tube was then sealed and the ligand-containing arm was immersed in an oil bath at 60°C while the other arm was maintained at ambient temperature [36, 42, 43]. After 5 days, crystals were deposited in the cooler arm and filtered off and dried in air. This complex was not soluble in DMSO or D_2O to provide an NMR spectrum. Yield 0.04 g, 22%; m.p. 173°C. – Analysis calcd. for $C_4H_8O_3PbS$ (343.35): C 13.99, H 2.35; found C 14.06, H 2.36%. – IR (KBr): $\nu = 3139$ m (O–H), $\nu_{as} = 2980$ m (CH_3), 2936 m (CH_2), $\nu_s = 2900$ m (CH_3), 2857 m (CH_2), $\nu_{as} = 1543$ s $(COO)^{OAc}$, $\nu_s = 1410$ s $(COO)^{OAc}$, $\delta_s = 1325$ (CH_2), $\nu = 1218$ (C–O), $\delta = 660$ $(OCO)^{OAc}$, $\nu = 620$ m (C–S) cm^{-1}.

4.4 Crystal structure determination

X-ray diffraction data for **1** were collected at $T = 173$ K using a Rigaku FR-X Ultrahigh Brilliance Microfocus RA generator/confocal optics with an XtaLAB P200 diffractometer. MoK_α radiation ($\lambda = 0.71075$ Å) was used and intensity data were collected using ω steps accumulating area detector images spanning at least a hemisphere of reciprocal space. All data were corrected for Lorentz polarization effects. A multiscan absorption correction was applied by using CrysAlis Pro [44]. The structure was solved using the intrinsic phasing method (Shelxt [45]) and refined by full-matrix least-squares against F^2 (Shelxl-2013 [46]). Nonhydrogen atoms were refined anisotropically, and H1 was refined freely from the electron density map, whilst all other hydrogen atoms were refined geometrically using a riding model. All calculations were performed using Olex 2 [47, 48]. Selected crystallographic data are presented in Table 1. Diagrams of the molecular structure were created using Shelxp [45] and Diamond [49]. Selected bond lengths are displayed in Table 2 and hydrogen bond geometries in Table 3.

CCDC 1884179 contains the supplementary crystallographic data for this paper. These data can be obtained free of charge from The Cambridge Crystallographic Data Centre via www.ccdc.cam.ac.uk/data_request/cif.

Table 1: Crystal structure data and structure refinement of complex **1**.

Empirical formula	$C_4H_8O_3PbS$
Formula weight, g mol^{-1}	343.35
Crystal size, mm^3	$0.33 \times 0.09 \times 0.06$
Temperature, K	173
Crystal system	Orthorhombic
Space group	*Pbca*
Unit cell dimensions	
a, Å	11.9624(5)
b, Å	6.1045(2)
c, Å	19.4074(9)
Volume, Å^3	1417.22(10)
Z	8
Calculated density, g cm^{-3}	3.22
Absorption coefficient, mm^{-1}	24.0
F(000), *e*	1232
θ range data collection, deg	2.703–28.780
h, *k*, *l* ranges	$-15 \le h \le 15$, $-8 \le k \le 7$, $-24 \le l \le 22$
Reflections collected/ independent/R_{int}	8892/1582/0.0311
Data/ref. parameters	1582/86
$R1/wR2$ ($I > 3\sigma(I)$)	0.0210/0.0555
$R1/wR2$ (all data)	0.0229/0.0561
Goodness-of-fit on F^2	1.075
Largest diff. peak/hole, *e* Å^{-3}	0.91/ – 1.33

Table 2: Selected bond lengths (Å) for complex **1** with estimated standard deviations in parentheses.[a]

Bond lengths	
Pb1–S1^{i}	3.1335(8)
Pb1–S1^{ii}	3.0643(9)
Pb1–S1	2.7541(12)
Pb1–O1	2.688(3)
Pb1–O2^{ii}	2.916(2)
Pb1–O2	2.661(2)
Pb1–O3	2.512(2)

[a]Symmetry operators: i: $1-x$, $0.5+y$, $1.5-z$; ii: $1.5-x$, $0.5+y$, z.

Table 3: Hydrogen bond dimensions (Å and deg) in complex **1**.[a]

D–H···A	*d*(D–H)	*d*(H···A)	*d*(D···A)	<(DHA)
O1–H1···O3^{i}	0.88(4)	1.78(4)	172(4)	2.660(4)

[a]Symmetry operators: i: $1-x$, $0.5+y$, $1.5-z$.

References

[1] R. F. Mendes, F. A. Almeida Paz, *Inorg. Chem. Front.* **2015**, *2*, 495–509.
[2] M. K. Smith, K. A. Mirica, *J. Am. Chem. Soc.* **2017**, *139*, 16759–16767.
[3] A. Nalaparaju, J. Jiang, *J. Phys. Chem.* **2012**, *C116*, 6925–6931.
[4] K. Markey, T. Putzeys, P. Horcajada, T. Devic, N. Guillou, M. Wübbenhorst, S. V. Cleuvenbergen, T. Verbiest, D. E. De Vos, M. A. Van Der Veen, *J. Chem. Soc. Dalton Trans.* **2016**, *45*, 4401–4406.
[5] E. Akbarzadeh, M. Falamarzi, M. R. Gholami, *Mater. Chem. Phys.* **2017**, *198*, 374–379.
[6] S. Kitagawa, *Angew. Chem. Int. Ed.* **2015**, *54*, 10686–10687.
[7] J. Goldsmith, A. G. Wong-Foy, M. J. Cafarella, D. J. Siegel, *Chem. Mater.* **2013**, *25*, 3373–3382.
[8] D. Alezi, Y. Belmabkhout, M. Suyetin, P. M. Bhatt, Ł. J. Weseliński, V. Solovyeva, K. Adil, I. Spanopoulos, P. N. Trikalitis, A.-H. Emwas, M. Eddaoudi, *J. Am. Chem. Soc.* **2015**, *137*, 13308–13318.
[9] C. V. Mcguire, R. S. Forgan, *Chem. Comm.* **2015**, *51*, 5199–5217.
[10] C. R. Pfeiffer, D. A. Fowler, J. L. Atwood, *CrystEngComm* **2015**, *17*, 4475–4485.
[11] M. Fernandez, A. S. Barnard, *ACS Comb. Sci.* **2016**, *18*, 243–252.
[12] C. Pettinari, F. Marchetti, N. Mosca, G. Tosi, A. Drozdov, *Polym. Int.* **2017**, *66*, 731–744.
[13] R. Feng, Y.-Y. Jia, Z.-Y. Li, Z. Chang, X.-H. Bu, *Chem. Sci.* **2018**, *9*, 950–955.
[14] M. Y. Masoomi, A. Morsali, P. C. Junk, J. Wang, *Ultrason. Sonochem.* **2017**, *34*, 984–992.
[15] M. Kurmoo, *Chem. Soc. Rev.* **2009**, *38*, 1353–1379.
[16] J. S. Miller, *Dalton Trans.* **2006**, 2742–2749.

[17] D. Tiana, C. H. Hendon, A. Walsh, *Chem. Comm.* **2014**, *50*, 13990–13993.
[18] P. Kar, R. Haldar, C. J. Gómez-García, A. Ghosh, *Inorg. Chem.* **2012**, *51*, 4265–4273.
[19] X.-Q. Wu, M.-L. Han, G.-W. Xu, B. Liu, D.-S. Li, J. Zhang, *Inorg. Chem. Commun.* **2015**, *58*, 60–63.
[20] R. L. Davidovich, V. Stavila, D. V. Marinin, E. I. Voit, K. H. Whitmire, *Coord. Chem. Rev.* **2009**, *253*, 1316–1352.
[21] T. Devic, C. Serre, *Chem. Soc. Rev.* **2014**, *43*, 6097–6115.
[22] L.-M. Wu, X.-T. Wu, L. Chen, *Coord. Chem. Rev.* **2009**, *253*, 2787–2804.
[23] H.-B. Duan, S.-S. Yu, S.-X. Liu, H. Zhang, *J. Chem. Soc. Dalton Trans.* **2017**, *46*, 2220–2227.
[24] A. M. Guloy, Z. Tang, P. B. Miranda, V. I. Srdanov, *Adv. Mater.* **2001**, *13*, 833–837.
[25] Z.-J. Huang, H.-J. Cheng, M. Dai, C.-Y. Ni, H.-X. Li, K.-P. Hou, Z.-G. Ren, J.-P. Lang, *Inorg. Chem. Commun.* **2013**, *31*, 33–36.
[26] H. Gao, G.-J. Yuan, Y.-N. Lu, S.-P. Zhao, X.-M. Ren, *Inorg. Chem. Commun.* **2013**, *32*, 18–21.
[27] Z.-K. Tan, R. S. Moghaddam, M. L. Lai, P. Docampo, R. Higler, F. Deschler, M. Price, A. Sadhanala, L. M. Pazos, D. Credgington, F. Hanusch, T. Bein, H. J. Snaith, R. H. Friend, *Nat. Nanotech.* **2014**, *9*, 687.
[28] J. A. Christians, R. C. M. Fung, P. V. Kamat, *J. Am. Chem. Soc.* **2014**, *136*, 758–764.
[29] Z. Mardani, V. Golsanamlou, Z. Jabbarzadeh, K. Moeini, S. Khodavandegar, C. Carpenter-Warren, A. M. Z. Slawin, J. D. Woollins, *J. Coord. Chem.* **2018**, *71*, 4109–4131.
[30] Z. Mardani, V. Golsanamlou, Z. Jabbarzadeh, K. Moeini, C. C. Warren, A. M. Z. Slawin, J. D. Woollins, *J. Korean Chem. Soc.* **2018**, *62*, 372–376.
[31] M. Hakimi, Z. Mardani, K. Moeini, E. Schuh, F. Mohr, *Z. Naturforsch.* **2013**, *68b*, 267–271.
[32] M. Hakimi, Z. Mardani, K. Moeini, F. Mohr, *Polyhedron* **2015**, *102*, 569–577.
[33] F. Marandi, K. Moeini, H. A. Rudbari, *Z. Naturforsch.* **2016**, *71b*, 959–965.
[34] K. Nakamoto, *Infrared and Raman Spectra of Inorganic and Coordination Compounds*, John Wiley, Hoboken, NJ, **2009**, p. 232.
[35] M. Hakimi, K. Moeini, Z. Mardani, F. Khorrami, *J. Korean Chem. Soc.* **2013**, *57*, 352–356.
[36] F. Marandi, K. Moeini, F. Alizadeh, Z. Mardani, C. K. Quah, W.-S. Loh, J. D. Woollins, *Inorg. Chim. Acta* **2018**, *482*, 717–725.
[37] L. Saghatforoush, K. Moeini, S. A. Hosseini-Yazdi, Z. Mardani, A. Hajabbas-Farshchi, H. T. Jameson, S. G. Telfer, J. D. Woollins, *RSC Adv.* **2018**, *8*, 35625–35639.
[38] F. H. Allen, *Acta Crystallogr.* **2002**, *B58*, 380–388.
[39] W. Clegg, I. L. Abrahams, C. D. Garner, *Acta Crystallogr.* **1984**, *C40*, 1367–1369.
[40] F. Marandi, K. Moeini, S. Ghasemzadeh, Z. Mardani, C. K. Quah, W.-S. Loh, *J. Mol. Struct.* **2017**, *1149*, 92–98.
[41] F. Marandi, K. Moeini, B. Mostafazadeh, H. Krautscheid, *Polyhedron* **2017**, *133*, 146–154.
[42] F. Marandi, F. Amoopour, I. Pantenburg, G. Meyer, *J. Mol. Struct.* **2010**, *973*, 124–129.
[43] F. Marandi, K. Moeini, A. Arkak, Z. Mardani, H. Krautscheid, *J. Coord. Chem.* **2018**, *71*, 3893–3911.
[44] CrysAlis Pro Software System (version 1.171.38.41), Intelligent Data Collection and Processing Software for Small Molecule and Protein Crystallography, Rigaku Oxford Diffraction, Yarnton, Oxfordshire (UK) **2015**.
[45] G. Sheldrick, *Acta Crystallogr.* **2015**, *A71*, 3–8.
[46] G. Sheldrick, *Acta Crystallogr.* **2015**, *C71*, 3–8.
[47] O. V. Dolomanov, L. J. Bourhis, R. J. Gildea, J. A. K. Howard, H. Puschmann, *J. Appl. Crystallogr.* **2009**, *42*, 339–341.
[48] L. J. Bourhis, O. V. Dolomanov, R. J. Gildea, J. A. K. Howard, H. Puschmann, *Acta Crystallogr.* **2015**, *A71*, 59–75.
[49] G. Bergerhof, M. Berndt, K. Brandenburg, *J. Res. Natl. Stand. Technol.* **1996**, *101*, 221–225.